Brain, Behavior, and Immunity 58 (2016) 107–117

Contents lists available at ScienceDirect

Brain, Behavior, and Immunity

journal homepage: www.elsevier.com/locate/ybrbi

Full-length Article

Spinal versus brain microglial and macrophage activation traits determine the differential neuroinflammatory responses and analgesic effect of minocycline in chronic neuropathic pain

Zhilin Li [a], Hong Wei [b], Sami Piirainen [a], Zuyue Chen [b], Eija Kalso [c], Antti Pertovaara [b], Li Tian [a,d,*]

[a] Neuroscience Center, University of Helsinki, Helsinki, Finland
[b] Department of Physiology, Faculty of Medicine, University of Helsinki, Helsinki, Finland
[c] Department of Pharmacology, Faculty of Medicine, University of Helsinki, Helsinki, Finland
[d] Psychiatry Research Center, Beijing Huilongguan Hospital, Peking University, Beijing, China

ARTICLE INFO

Article history:
Received 13 April 2016
Received in revised form 25 May 2016
Accepted 31 May 2016
Available online 1 June 2016

Keywords:
Neuropathic pain
Spared nerve injury
Spinal cord
Prefrontal cortex
Microglia/macrophages
Minocycline

ABSTRACT

Substantial evidence indicates involvement of microglia/macrophages in chronic neuropathic pain. However, the temporal-spatial features of microglial/macrophage activation and their pain-bound roles remain elusive. Here, we evaluated microglia/macrophages and the subtypes in the lumbar spinal cord (SC) and prefrontal cortex (PFC), and analgesic-anxiolytic effect of minocycline at different stages following spared nerve injury (SNI) in rats. While SNI enhanced the number of spinal microglia/macrophages since post-operative day (POD)3, pro-inflammatory MHCII$^+$ spinal microglia/macrophages were unexpectedly less abundant in SNI rats than shams on POD21. By contrast, less abundant anti-inflammatory CD172a (SIRPα)$^+$ microglia/macrophages were found in the PFC of SNI rats. Interestingly in naïve rats, microglial/macrophage expression of CD11b/c, MHCII and MHCII$^+$/CD172a$^+$ ratio were higher in the SC than the cortex. Consistently, multiple immune genes involved in anti-inflammation, phagocytosis, complement activation and M2 microglial/macrophage polarization were upregulated in the spinal dorsal horn and dorsal root ganglia but downregulated in the PFC of SNI rats. Furthermore, daily intrathecal minocycline treatment starting from POD0 for two weeks alleviated mechanical allodynia most robustly before POD3 and attenuated anxiety on POD9. Although minocycline dampened spinal MHCII$^+$ microglia/macrophages until POD13, it failed to do so on cortical microglia/macrophages, indicating that dampening only spinal inflammation may not be enough to alleviate centralized pain at the chronic stage. Taken together, our data provide the first evidence that basal microglial/macrophage traits underlie differential region-specific responses to SNI and minocycline treatment, and suggest that drug treatment efficiently targeting not only spinal but also brain inflammation may be more effective in treating chronic neuropathic pain.

1. Introduction

Neuropathic pain is a complex pain state caused by dysfunction of the somatosensory nervous system, starting from primary nociceptive afferent axons up to various supraspinal brain regions. Most cases of neuropathic pain are chronic and patients often develop comorbidities such as anxiety, depression and sleep disturbance, which in turn contribute to or exacerbate pain (Nicholson and Verma, 2004; Page et al., 2014). Several experimental rodent models, such as spared nerve injury (SNI), have been used to study neuropathic pain and its comorbidities (Campbell and Meyer, 2006). With these rodent models, glial cells, including astrocytes and microglia, and neuron-glial interactions have been appreciated in the development and maintenance of neuropathic pain (Benarroch, 2010; Graeber and Christie, 2012; Grace et al., 2014). However, whether subtypes of glial cells play cohesive or counteracting roles in neuropathic pain is so far elusive (Tanga et al., 2004; Herrera-Molina and von Bernhardi, 2005; Milligan and Watkins, 2009).

It has been suggested that proportions of glial cells that colonize the central nervous system (CNS) vary a lot across different regions, which may be affected and affect physiological functions

* Corresponding author at: Neuroscience Center, University of Helsinki, Viikinkaari 4, FIN-00014 Helsinki, Finland.
E-mail addresses: zhilin.li@helsinki.fi (Z. Li), hong.wei@helsinki.fi (H. Wei), sami.piirainen@helsinki.fi (S. Piirainen), zuyue.chen@helsinki.fi (Z. Chen), eija.kalso@helsinki.fi (E. Kalso), antti.pertovaara@helsinki.fi (A. Pertovaara), li.tian@helsinki.fi (L. Tian).

http://dx.doi.org/10.1016/j.bbi.2016.05.021
0889-1591/

of neighboring neurons (Herculano-Houzel, 2014). Such a difference in physiological function has recently been demonstrated for astrocytes in the brain (Kasymov et al., 2013; Schitine et al., 2015). As for microglia, despite some observations demonstrating their diversities in abundancy, morphology and molecular feature in different regions of the CNS (Lawson et al., 1990; Savchenko et al., 1997; Olson, 2010; Doorn et al., 2015; Grabert et al., 2016), it is currently unclear what biological effects such differences may render on neurons in a healthy or diseased condition. Particularly, whether they play homo- or heterogeneous roles in sensitization of chronic neuropathic pain has not been addressed so far.

Similar to the classical M1 versus the alternative M2 paradigm defined for macrophages, M1/M2 microglial polarization has been recently coined and characterized in various CNS disorders (Franco and Fernandez-Suarez, 2015; Hu et al., 2015), including neuropathic pain (Popiolek-Barczyk et al., 2015; Xu et al., 2016). We have also investigated M1/M2 microglial polarization in several experimental animal models, including anxiety (Li et al., 2014) and epilepsy (Okuneva et al., 2015). M1 microglia upregulate several co-stimulatory molecules, including major histocompatibility complex class II (MHCII) that is important for antigen presentation, and secret pro-inflammatory mediators, thereby exacerbating neuronal damage. In contrast, M2 microglia secret cellular factors to dampen inflammation and phagocytoze cell debris to promote tissue repair (Franco and Fernandez-Suarez, 2015; Hu et al., 2015). Microglia can normally maintain an M2-like quiescent/homeostatic state via constitutively expressing cell surface receptors (e.g. CD172a (SIRPα), CX_3CR_1 and CD200R) that receive contact-dependent inhibitory/deactivating signals from their respective ligands (e.g. CD47, CX_3CL_1 and CD200) expressed by neurons (Carson et al., 2007; Ransohoff and Cardona, 2010; Saijo and Glass, 2011; Cherry et al., 2014; Hu et al., 2014). Cumulative evidence shows that M2 microglia contribute to neuroprotection in CNS injuries or diseases by upregulation of such receptors (Franco and Fernandez-Suarez, 2015; Hu et al., 2015). CD172a, which is an M2 marker and carries an inhibitory immunoreceptor tyrosine-based inhibition motif (ITIM) in its cytoplasmic tail, functions to limit activation of other immune signaling receptors that contribute to inflammation (Linnartz and Neumann, 2013) and was previously used to characterize microglia in several pain models (Blackbeard et al., 2007).

Currently available pain-relievers are not universally effective and often lack long-lasting efficacy due to development of analgesic tolerance. So far, most studies have considered microglia to play mainly a detrimental role and have targeted microglial activation for relieving neuropathic pain (Milligan and Watkins, 2009; Aldskogius and Kozlova, 2013; Tsuda et al., 2013). As a potent microglial inhibitor, minocycline was previously demonstrated to alleviate chronic neuropathic pain (Chang and Waxman, 2010; Willemen et al., 2010). However, other studies on its analgesic effects have given mixed results. Some reported that minocycline prevented the development of, but failed to reverse the existing, mechanical allodynia in various neuropathic pain models (Raghavendra et al., 2003; Ledeboer et al., 2005; Sung et al., 2012; Yamamoto et al., 2015), while two other studies recently showed that minocycline pretreatment had no effect on mechanical allodynia (Burke et al., 2014; Taylor et al., 2015). A clear explanation on these discrepancies is currently lacking, due to insufficient knowledge on the nature of microglial activation and the mechanisms of minocycline in controlling microglia in neuropathic pain models. These knowledge gaps call for a more thorough investigation on microglia in injury- and drug-response in order to improve the efficacy of not only minocycline but also other anti-inflammatory analgesics (Benarroch, 2010; McMahon et al., 2015).

In this study, we aim to better understand the temporal-spatial roles that microglia/macrophages may play during the course of chronic neuropathic pain, and to analyze the mechanisms underlying the efficacies of minocycline on attenuating mechanical allodynia and comorbid anxiety-like behaviors of rats following SNI.

2. Materials and methods

2.1. Animals

Adult male Hannover-Wistar rats weighing 250–300 g were purchased from Envigo (Horst, Netherlands). Rats were single-housed in a 12-h light/dark cycle with food and water *ad libitum*. Experiments were performed during the light cycle. Experiment procedures were approved by the Experimental Animal Ethics Committee of the Provincial Government of Southern Finland, and performed according to the guidelines of European Communities Council Directive (2010/63/EU). All efforts were made to limit distress and to use minimal number of animals required to produce scientifically reliable data.

2.2. SNI surgery

To induce neuropathic pain in rats, SNI model was adopted (Decosterd and Woolf, 2000). Prior to surgery, a rat was anesthetized with 60 mg/kg body weight (BW) of intraperitoneally (i.p.) injected sodium pentobarbital (Orion Pharma, Espoo, Finland). An incision was subsequently made into the skin on the lateral surface of the left thigh, followed by a section through the biceps femoris muscle to expose the sciatic nerve and its terminal branches: the sural, common peroneal and tibial nerves. The common peroneal and tibial nerves were then tightly ligated with 4–0 silk and sectioned at sites distal to the ligation. 3–4 mm of the distal nerve stumps were then removed. The sural nerve was left intact and care was taken not to stretch it. For the sham-operated rats, the sciatic nerve was exposed in the same way but not ligated. To prevent post-operative pain, animals were treated with 0.01 mg/kg BW of buprenorphine twice daily for three days, which was a mandatory procedure according to the ethical permission.

2.3. Neuropathic pain- and anxiety-like behavioral tests

Before assessment of neuropathic pain-like behavior, rats were habituated to an experimental room for at least three consecutive days, one hour per day. Mechanical allodynia was assessed by a calibrated series of von Frey monofilaments producing forces ranging from 0.4 to 60 g (0.4, 1, 2, 4, 6, 8, 10, 15, 26 and 60 g, North Coast Medical Inc, Morgan Hill, CA). During the test, a rat was placed on a grid and allowed to move freely inside a transparent box. The monofilaments below the grid were applied to a hind paw of the rat with increasing forces until the rat withdrew it. The ipsilateral hind paw was stimulated for five times at each stimulus force with an ascending series of the monofilaments. At each stimulus force, the number of withdrawal responses was counted, and the withdrawal response rate (%) was calculated. An increase in the withdrawal response rate was considered to represent neuropathic pain-like mechanical hypersensitivity.

In a light-dark (LD) or open field (OF) test, rats were transported into an experimental room for one-hour adaptation. The LD test was carried out in an experimental arena consisting of two compartments (each 26.4 × 20.6 cm), one of which was dark and the other illuminated. Dark and light compartments were connected by a dark central chamber (15.9 × 20.6 cm) with open doors to allow free movement of a rat between the compartments. A rat was released to the light compartment and allowed to explore the experimental chamber for 10 min. Time spent in each compart-

ment and number of fecal boli excreted during the test were counted. In the OF test, a rat was placed inside facing the wall of a round chamber (diameter 85 cm) and its movement was video-tracked for 5 min. Time spent in the central (diameter 51 cm) or peripheral areas was calculated.

2.4. Immunohistochemistry (IHC)

Rats were deeply anesthetized with sodium pentobarbital and perfused intracardially with PBS followed by 4% paraformaldehyde in PBS. The lumbar (L4-6) spinal cord (SC)s were then carefully dissected and submersed into 4% PFA for overnight post-fixation. The SCs were transferred to 30% sucrose in PBS for dehydration, and were finally frozen in Tissuetek (Sakura) and cut into 20 μm floating sections. Cryosections were blocked with 5% goat serum and permeabilized with 0.1% Tween-20 in TBS and incubated with a rabbit anti-Iba1 polyclonal antibody (Wako Chemical, Japan), followed by an Alexa Fluor 568-conjugated goat anti-rabbit IgG antibody (Life Technologies). Stained sections were mounted onto glass slides and imaged by a Zeiss Axioplan 2 microscope under the 10× magnitude and an Axiocam HR camera (Carl Zeiss).

2.5. Flow cytometry

Rats were deeply anesthetized with sodium pentobarbital and perfused intracardially with PBS. The tissues were dissected, weighed, cut into tiny pieces and gently homogenized through 70 μm cell strainers (Fisher Scientific) in PBS/1% FCS/0.02% NaN_3. Single cell suspensions prepared from ~25 mg tissue per sample were blocked with 5% normal rat serum, and stained with a combination of anti-rat flow cytometric markers, including Granulocyte-FITC (clone HIS48, eBioscience), CD172a-PE (clone OX41, BioLegend), MHCII-PerCP-eFluor 710 (clone OX17, eBioscience), and CD11b/c-eFluor 660 (clone OX42, eBioscience) with light protection at 4 °C under a 60-min continuous rotation. Specificities of flow cytometric markers were confirmed by comparing with respective isotype controls. After washing, cells were resuspended into 2 ml PBS/1% FCS/0.02% NaN_3 buffer, and acquired on a 2-laser, 6-color Gallios cytometer (Beckman Coulter) under a live gate of $CD11b/c^+$. Flow cytometric data were analyzed with the Kaluza flow analysis 1.3 software (Beckman Coulter). Microglia/macrophages were defined as $CD11b/c^+Granulocyte^-$ total, $MHCII^+$ and $CD172a^+$ subtypes. Cell populations were calculated and presented as numbers of cells per mg tissue, percentages among total microglia/macrophages, or $MHCII^+/CD172a^+$ microglial/macrophage ratios.

2.6. Total RNA purification and RT-qPCR

Total RNAs from dissected tissues of surgerized rats were extracted by using a GeneJET RNA Purification Kit (Thermo Scientific), treated with TURBO DNA-free DNase (Ambion) to remove trace amount of genomic DNA, and reversely transcribed (200 ng) with a RevertAid First Strand cDNA Synthesis Kit (Thermo Scientific). RT-qPCR was performed by using corresponding primers and Maxima SYBR Green qPCR Master Mix (Thermo Scientific) on a CFX384 Real-Time PCR Detection System (Bio-Rad). The forward and reverse primers used for target genes are listed in Table S1. Quantification for each gene was performed by normalization with a housekeeping gene *Actb*, and represented as fold change via the ΔΔCt method.

2.7. Chronic intrathecal minocycline administration

Rats were implanted with an intrathecal catheter (PE-10; Becton, Dickinson and Company, Sparks, MD, USA) under general anesthesia (sodium pentobarbital 60 mg/kg i.p.) and randomly assigned to two groups. Starting from the operation day and 20 min before SNI surgery, one group (post-operative day (POD) 3: n = 5; POD13: n = 5) received 50 μg intrathecal (i.t.) minocycline hydrochloride (Sigma-Aldrich) daily for 14 consecutive days, another group (POD3: n = 6; POD13: n = 5) received the same volume of saline. Von Frey hair test was performed both on the operation day prior to surgery and regularly during POD1-13.

2.8. Statistical analysis

Data were analyzed by one-way, ordinary or mixed-design two-way analysis of variance (ANOVA) with Bonferroni's *post hoc* or Fisher's LSD test. Two group comparison was done with Student's *t* test. All values presented were mean ± standard error of mean (SEM). Statistical significance was set to $p < 0.05$. *P* values were classified as $^{*}p < 0.05$, $^{**}p < 0.01$, $^{***}p < 0.001$.

3. Results

3.1. Induction of neuropathic pain-like mechanical allodynia and anxiety-like behaviors in rats following SNI

To verify development of neuropathic pain-like mechanical hypersensitivity in rats, we assessed the ipsilateral hind paw withdrawal responses both prior to and after SNI surgery (Fig. 1A). SNI induced a marked and prolonged mechanical allodynia, as reflected by a higher hind paw withdrawal response rate at the stimulus force of 6 g in SNI rats as compared to Sham at both acute (POD3) and chronic (POD6 and 20) stages (Fig. 1B). In addition, SNI rats excreted higher numbers of fecal boli in a light-dark test within POD20 (Fig. 1C), suggesting a potency of time-dependent development of anxiety-like behavior.

3.2. Enhanced number of microglia/macrophages in the ipsilateral lumbar SC of SNI rats

It was demonstrated that robust microgliosis occured at early stages in ipsilateral spinal DH that may last long following a peripheral nerve injury (Echeverry et al., 2008). In our study, we also checked microglial/macrophage density in the lumbar SCs of SNI rats on POD7 and POD21 by IHC with an antibody against Iba1. As expected, SNI induced massive focal increases of microglia/macrophages in the dorsal and ventral horns of ipsilateral lumbar SC (Fig. 1D).

Due to the limitation of IHC in characterizing molecular features of activated microglia/macrophages, and in order to quantify the number of microglia/macrophages and simultaneously characterize their polarization profiles in the CNS (SC and brain) of SNI rats, we further set up a flow cytometry-based approach using a combination of anti-rat flow cytometry markers. This enabled us to measure total number of microglia/macrophages, their subpopulations ($MHCII^+$ and $CD172a^+$ microglia/macrophages), as well as microglial/macrophage surface expression levels (mean fluorescent intensity (MFI)) of inflammatory markers including CD11b/c, MHCII and CD172a (Gating strategies for the SC and brain microglia/macrophages are shown in Figs. 2A and 3A, respectively). When comparing total numbers of microglia/macrophages, we found a profound increased number of microglia/macrophages in the ipsilateral lumbar SCs of SNI rats as compared to Sham, particularly on POD7 and 21 (Fig. 2B), whereas no such difference was observed in the contralateral lumbar SCs (data not shown). The number of microglia/macrophages was steadily intensified along with time in SNI rats (POD21 vs POD3: $p = 0.0009$), but not in Sham (Fig. 2B). In addition, we found higher microglial/macrophage

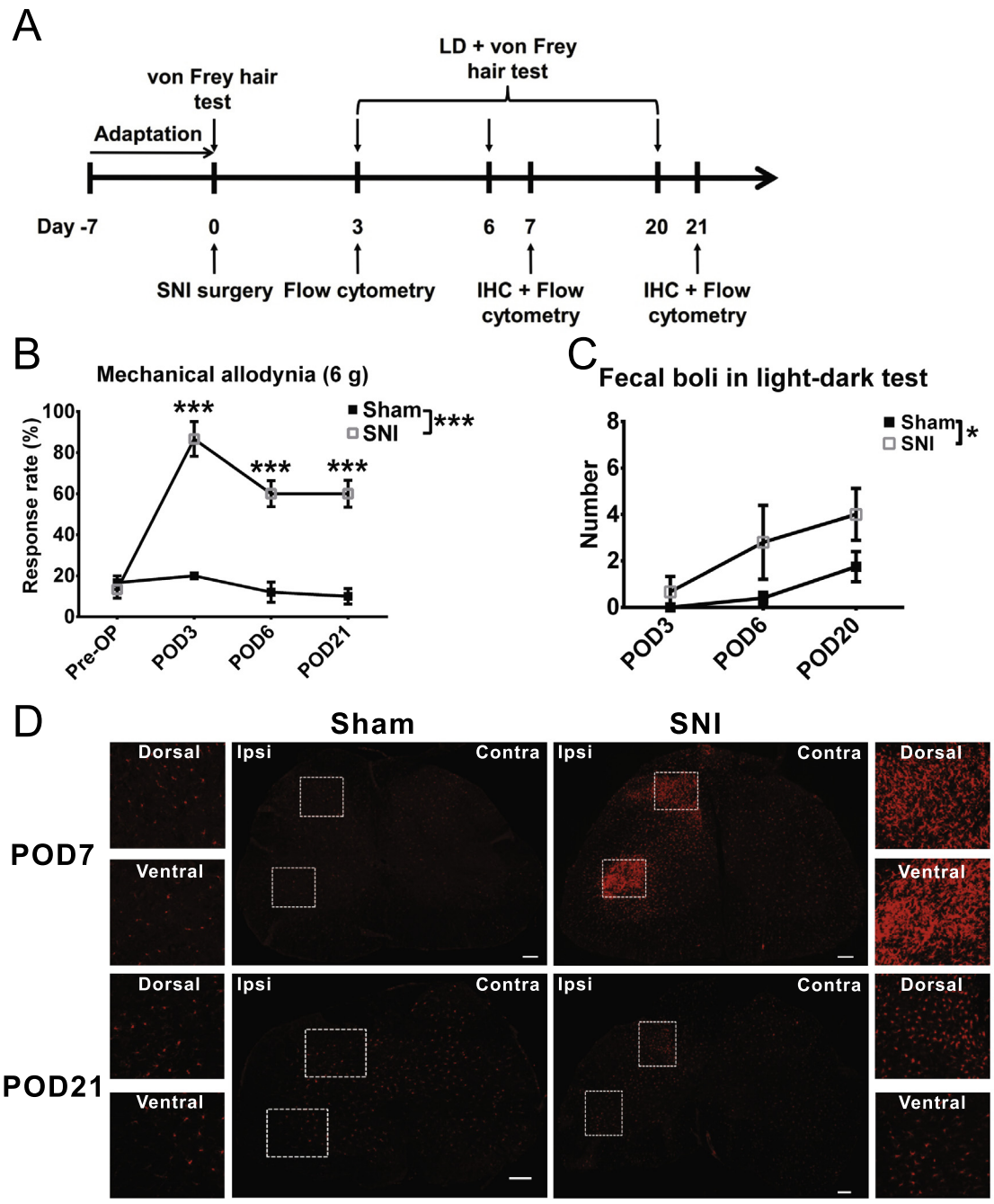

Fig. 1. SNI induces mechanical allodynia, anxiety-like behavior and spinal microgliosis in rats. Pre-OP: Sham = 6, SNI = 6; POD3: Sham = 6, SNI = 6; POD6: Sham = 5, SNI = 5; POD20: Sham = 8, SNI = 8. (A) A flow chart illustrates the experimental procedure. (B) Ipsilateral hind paw withdrawal response rate evoked by von Frey monofilament stimulation at the force of 6 g demonstrated enhanced mechanical allodynia in SNI as compared to Sham within POD20 (group effect: $F(1,42) = 111.0$, $p < 0.0001$; time effect: $F(3,42) = 16.55$, $p < 0.0001$; group × time interaction: $F(3,42) = 15.57$, $p < 0.0001$). (C) Numbers of fecal boli excreted in a light-dark (LD) box were higher in SNI than Sham within POD20 in a time-dependent manner, indicating the development of an anxiety-like behavior (group effect: $F(1,32) = 5.791$, $p = 0.0221$; time effect: $F(2,32) = 4.488$, $p = 0.0191$). Data were analyzed by a two-way ANOVA with Bonferroni's *post hoc* test and presented as mean ± SEM. $^{*}p < 0.05$, $^{***}p < 0.001$. (D) Immunostaining images represent Iba-1^{+} microglia (shown in red) in both ipsi and contra lumbar SCs of Sham and SNI rats on POD7 and POD21. Scale bar = 200 μm.

CD11b/c expression, particularly on POD21 in the lumbar SCs of SNI rats (Fig. 2C).

3.3. Differential microglial/macrophage polarization between the ipsilateral lumbar SC and the contralateral prefrontal cortex (PFC) on POD21 following SNI

To gain more insights into the temporal and spatial microglial/macrophage polarization profiles induced by SNI, we next compared microglial/macrophage subpopulations on POD3, 7 and 21. On POD3, although increased number of spinal microglia/macrophages was obvious as above-mentioned, barely no difference between SNI and Sham rats was observed with regard to the percentages of MHCII^{+} and CD172a^{+} microglia/macrophages in the ipsilateral lumbar SCs (Fig. 2D and E). However, on POD21, the MHCII^{+} microglia/macrophages was less abundant in SNI than Sham (Fig. 2D). By contrast, while percentages of CD172a^{+} microglia/macrophages only fluctuated with time but remained unchanged between SNI and Sham (Fig. 2E), quantification of cell numbers of MHCII^{+} (Fig. S1A) and CD172a^{+} (Fig. S1B)

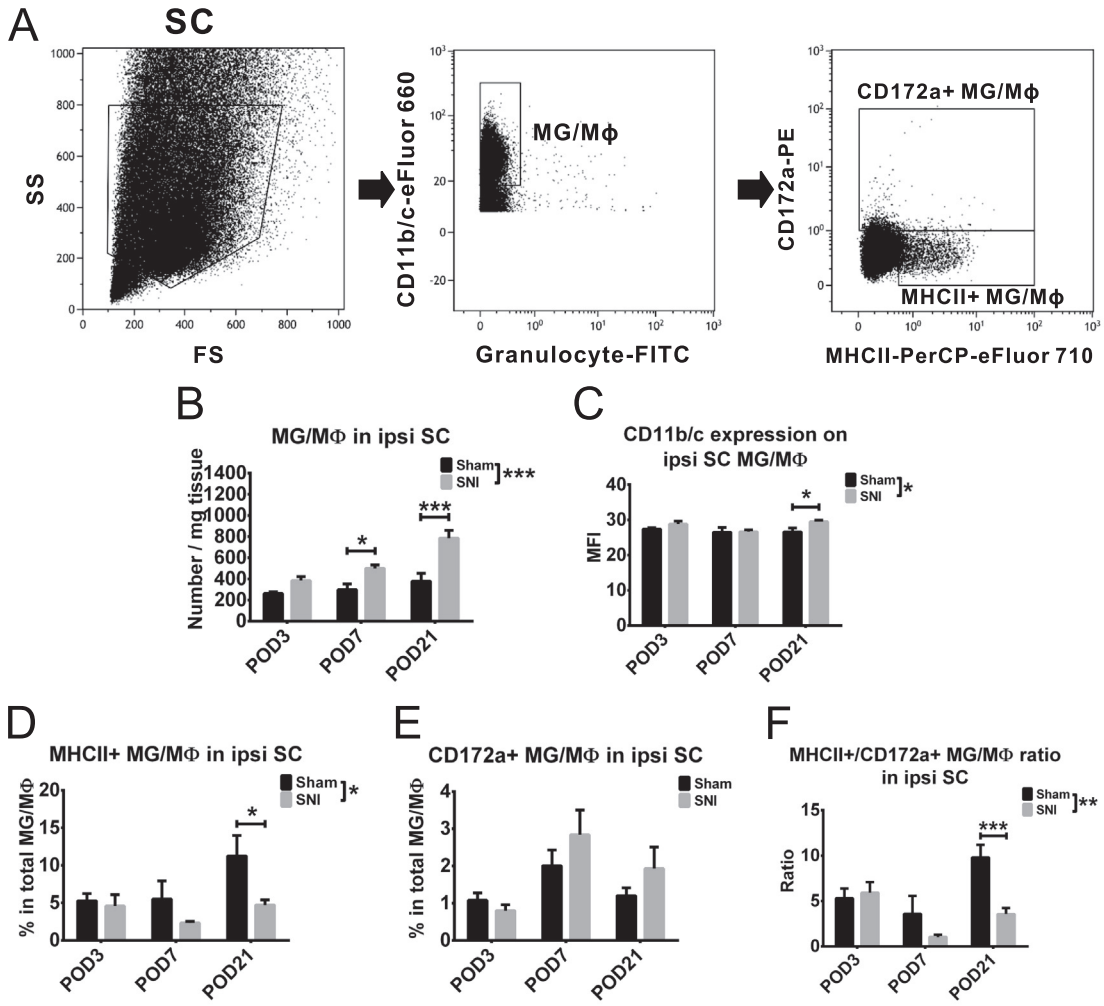

Fig. 2. Enhanced number of MG/MΦ and a lower percentage of pro-inflammatory MG/MΦ in the ipsilateral lumbar SC of SNI rats. POD3: Sham = 6, SNI = 6; POD7: Sham = 5, SNI = 5; POD21: Sham = 8, SNI = 8. Single cell suspensions of spinal tissues were stained with a combination of anti-rat flow cytometric cell surface markers. (A) Total MG/MΦ ($CD11b/c^{+}Granulocyte^{-}$) and MG/MΦ subtypes ($MHCII^{+}$ versus $CD172a^{+}$ MG/MΦ) are shown in flow cytometric plots. (B) Numbers of total MG/MΦ normalized to tissue weight (mg) were increased during POD3-21 and were more abundant in SNI than Sham, particularly on POD7 and POD21 (group effect: $F(1,32) = 23.46$, $p < 0.0001$; time effect: $F(2,32) = 10.78$, $p = 0.0003$). (C) MG/MΦ CD11b/c mean fluorescent intensity (MFI) was higher in SNI than Sham, particularly on POD21 (group effect: $F(1,32) = 4.389$, $p = 0.0442$). (D–E) Percentages of $MHCII^{+}$ and $CD172a^{+}$ MG/MΦ were measured. The percentages of $MHCII^{+}$ MG/MΦ were lower in SNI as compared to Sham, particularly on POD21 (D, group effect: $F(1,32) = 5.409$, $p = 0.0265$), whereas $CD172a^{+}$ MG/MΦ showed only time-dependent changes but no group effect (E, time effect: $F(2,32) = 5.352$, $p = 0.0099$). $MHCII^{+}/CD172a^{+}$ MG/MΦ ratio was lower in SNI as compared to Sham, particularly on POD21 (F, group effect: $F(1,32) = 7.551$, $p = 0.0098$; time effect: $F(2,32) = 6.701$, $p = 0.0037$; group × time interaction: $F(2,32) = 4.543$, $p = 0.0183$). Data were analyzed by a two-way ANOVA with Fisher's LSD or Bonferroni's *post hoc* test and presented as mean ± SEM. $^{*}p < 0.05$, $^{**}p < 0.01$, $^{***}p < 0.001$.

microglia/macrophages in the SC showed a higher number of $CD172a^{+}$ microglia/macrophages in SNI than Sham, resulting in a lower $MHCII^{+}/CD172a^{+}$ microglial/macrophage ratio (regarded as a pro- versus anti-inflammatory index) in SNI than Sham, particularly on POD21 (Fig. 2F). This index also showed an ascent in Sham (POD21 vs POD3: $p = 0.0319$) but not in SNI (POD21 vs POD3: $p = 0.0916$) during POD3-21 (Fig. 2F). Given the inflammation-dampening function of CD172a, these data suggest that increased number of spinal microglia/macrophages may not necessarily be always harmful in the course of SNI, and furthermore, although microglia/macrophage propagation occurs at an early stage, sufficient time may be required for microglia/macrophages to get ready to exert their anti-inflammatory roles to protect neurons.

We previously reported that microglial M1/M2 polarization was affected by anxiety trait in mice (Li et al., 2014). Since we found that SNI rats were more nervous here, we also characterized microglial/macrophage polarization in the contralateral PFC, which is sensitized by pain besides regulating anxiety. At the early SNI stages (POD3 and 7), no apparent microglial/macrophage responses were found (Fig. 3B–D). However, on POD21 and in an intriguing contrast to spinal microglia/macrophages, percentages of $MHCII^{+}$ microglia/macrophages remained unchanged in the PFC (Fig. 3B, normalized cell number shown in Fig. S1C). In addition, percentages of prefrontal $CD172a^{+}$ microglia/macrophages were lower in SNI than Sham (Fig. 3C, normalized cell number shown in Fig. S1D). Percentages of prefrontal $MHCII^{+}$ and $CD172a^{+}$ microglia/macrophages were increased in both SNI and Sham groups along with time during POD3-21 (Fig. 3B and C). Moreover, a lower microglial/macrophage CD172a expression in SNI on POD21 was also noticed (Fig. 3D). These data indicate that at the later stage of SNI, unlike spinal microglia/macrophages, cortical microglia/macrophages may show a pronounced reduction in the CD172a-mediated dampening of pro-inflammatory response.

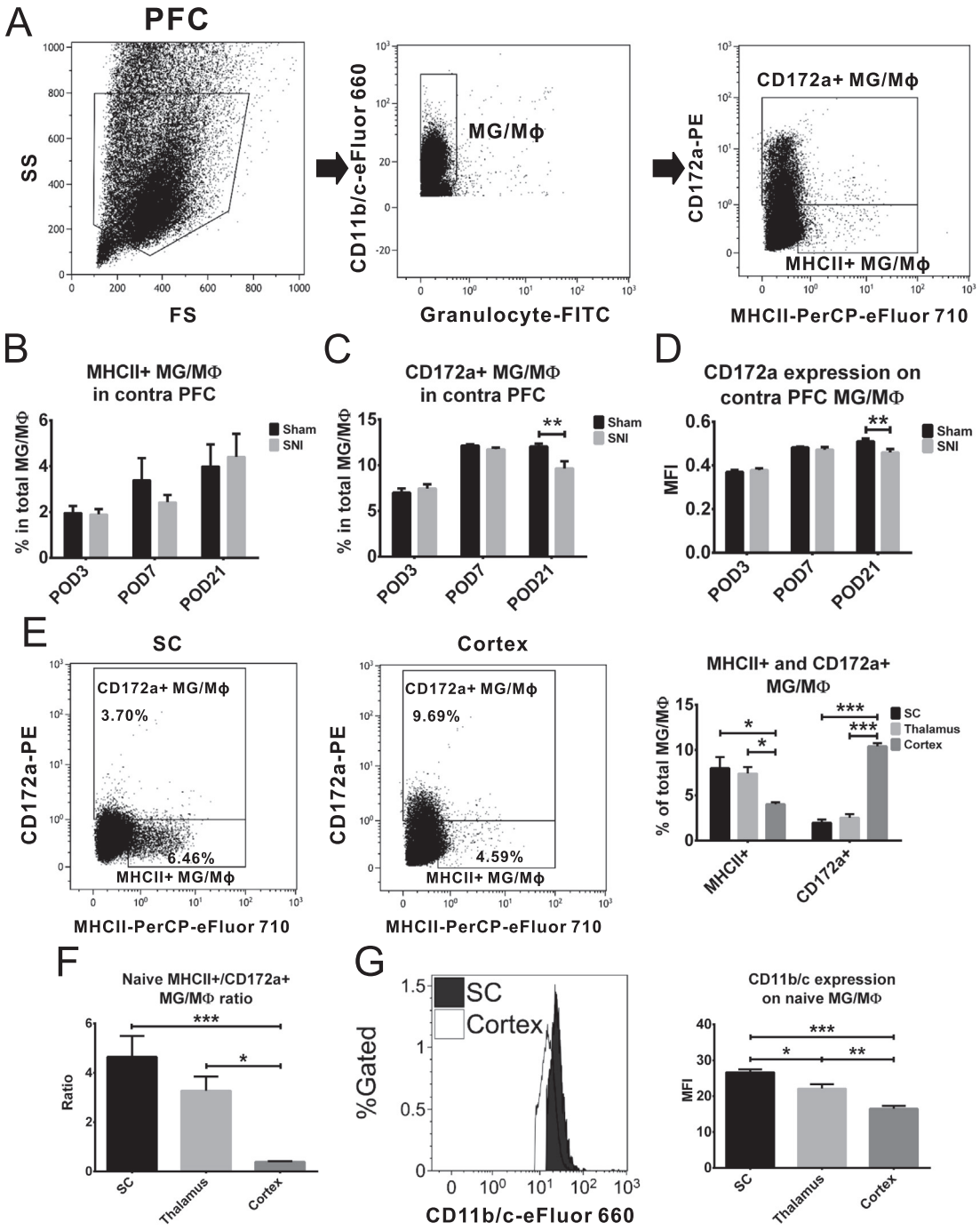

Fig. 3. A lower percentage of anti-inflammatory MG/MΦ in the contralateral PFC of SNI rats on POD21 and a stronger inflammatory trait of spinal than brain MG/MΦ in naïve rats. POD3: Sham = 6, SNI = 6; POD7: Sham = 5, SNI = 5; POD21: Sham = 8, SNI = 8. (A) Total MG/MΦ and their subtypes are shown in flow cytometric plots. (B–C) Percentages of MHCII$^+$ and CD172a$^+$ MG/MΦ were measured. The percentages of MHCII$^+$ MG/MΦ (B, time effect: $F(2,32) = 4.394$, $p = 0.0206$) and CD172a$^+$ MG/MΦ (C, time effect: $F(2,32) = 41.48$, $p < 0.0001$; group × time interaction: $F(2,32) = 4.432$, $p = 0.0200$), and MG/MΦ CD172a mean fluorescent intensity (MFI) (D, time effect: $F(2,32) = 48.51$, $p < 0.0001$; group × time interaction: $F(2,32) = 3.340$, $p = 0.0481$) were increased during POD3-21. However, the percentage of CD172a$^+$ MG/MΦ (C) and MG/MΦ CD172a MFI (D) were lower in SNI than Sham on POD21. (E-G) Basal immune statuses of spinal, thalamic and cortical MG/MΦ in naïve rats (n = 6) were studied by flow cytometry. (E) MHCII$^+$ MG/MΦ was relatively more abundant in the SC than brain ($F(2,15) = 6.713$, $p = 0.0083$), while a prominent opposite phenomenon was true for CD172a$^+$ MG/MΦ ($F(2,15) = 160.4$, $p < 0.0001$), resulting in a higher spinal MHCII$^+$/CD172a$^+$ MG/MΦ ratio in the SC than brain (F, $F(2,15) = 13.46$, $p = 0.0004$). (G) Representative overlay histogram plot showing MFIs of MG/MΦ CD11b/c between SC and cortex is presented. MFI of CD11b/c was higher in the SC than brain ($F(2,15) = 30.00$, $p < 0.0001$). Data were analyzed by a one- or two-way ANOVA with Bonferroni's *post hoc* test and presented as mean ± SEM. $^*p < 0.05$, $^{**}p < 0.01$, $^{***}p < 0.001$.

3.4. Differential basal inflammatory profiles between the SC and the brain of naïve rats

To figure out possible explanations why spinal and cortical microglia/macrophages showed intriguingly opposite responses to SNI, we compared their immune profiles in naïve rats by flow cytometry. Interestingly, microglial/macrophage cell numbers were less abundant in the lumbar SC than the thalamus and cortex (Fig. S2A). Regarding microglial/macrophage subtypes, we found that MHCII$^+$ microglia/macrophages were more abundant (Fig. 3E),

while CD172a$^+$ microglia/macrophages were profoundly less abundant (Fig. 3E), making the MHCII$^+$/CD172a$^+$ microglial/macrophage ratio higher in the lumbar SC than the cortex (Fig. 3F). In addition, lumbar spinal microglia/macrophages expressed higher levels of CD11b/c (Fig. 3G) and MHCII (Fig. S2B) than the cortical microglia/macrophages. Thalamic microglia/macrophages fell in between spinal and cortical microglia/macrophages with regard to most of the above immune parameters (Figs. 3E–G and S2B). These data clearly demonstrate that basal immuno-statuses of microglia/macrophages are different across different CNS regions.

Additionally, when exploring transcriptomic data of the brain and SC in GEO database, we detected clusters of immune genes that were differentially expressed between these two regions, such as *Cx3cl1* and *Rt1-da*, or across different brain regions (e.g. amygdala, cortex, hippocampal CA1 and CA3) of naïve adult rats, such as *Ccr2*, *Csf1*, *Rt1-dma*, *Tgfb1* and *Tnfsf11* (Table S2). These data further suggest that basal immune status in the CNS is region-specific and it may underlie regionally different microglial/macrophage responses to SNI.

3.5. Upregulation of anti-inflammatory, M2 and phagocytic genes in the lumbar spinal dorsal horn (DH) and dorsal root ganglia (DRG), and their downregulation in the PFC and primary somatosensory cortex (PSC) induced by SNI on POD7

To investigate what genes may be involved in the development of neuropathic pain, we explored the GEO microarray datasets reported by Costigan et al., who have used the same SNI paradigm in adult male rats and analyzed the DHs of both sham and SNI rats on POD7 (Costigan et al., 2009). By comparing these microarray datasets, we found a majority of differentially expressed genes are involved in the immune responses, such as regulation of immune responses to stimulus, antigen processing and presentation, and phagocytosis (Table S3 and Fig. S3A).

Bearing this knowledge and based on the common acknowledgement of cytokines and M1/M2 microglia/macrophage markers, we selected a list of microglia/macrophage-related immune genes for a further analysis. These include microglial/macrophage activation marker *Cd68*, major inhibitory Fcγ receptor *Fcgr2b* (Anthony and Ravetch, 2010), phagocytic receptor *Mrc1*, pro- versus anti-inflammatory cytokines/mediators (*Il1b*, *Il10*, *Tnf* and *Tgfb1*), M1/M2 microglia/macrophage signature genes (*Nos2* and *Arg1*) and complement genes (*C1qb*, *C3* and *C4a*). Beforehand, we first measured their gene expressions in the lumbar SC, thalamus and PFC of naïve rats. Interestingly, we again found basal regional differences, such that mRNA levels of genes involved in complement activation, microglial/macrophage phagocytosis and M2 activation were higher in the lumbar SC than PFC, while pro- or anti-inflammatory cytokines showed no differences (Fig. 4A).

We next inquired how these genes may respond to SNI in the SC versus the brain. We therefore measured their mRNA expressions in the ipsilateral lumbar DH and DRG, and the contralateral PFC and PSC of both SNI and Sham rats on POD7. Notably, we found higher mRNA levels of *Cd68* and *Tgfb1* in the DH of SNI as compared to Sham (Fig. 4B), while *Il1b* and *Tnf* remained unchanged (data not shown). Furthermore, *C1qb*, *C3* and *C4a* were all higher in the DH of SNI rats (Fig. 4B). Although DRG is devoid of microglia, macrophages have been shown to infiltrate there in response to nerve injury (Komori et al., 2011). Therefore, we also investigated expression of the above genes in the ipsilateral DRG. Similar to the DH, *Fcgr2b*, *Tgfb1*, *C1qb*, *C3* and *C4a* were all higher in the ipsilateral DRG of SNI rats (Fig. 4C). By contrast, *Cd68*, *Fcgr2b*, *Tgfb1*, *C1qb*, *C3* and *C4a* were all notably lower in the contralateral PFC of SNI rats (Fig. 4D). We further measured *Nos2* and *Arg1* in the ipsilateral DRG and contralateral PFC. Although *Nos2* remained unchanged (Fig. 4E), *Arg1* was predominantly higher (Fig. 4F), making *Nos2*/*Arg1* ratio lower in the ipsilateral DRG of SNI rats than in Sham (Fig. 4G). Furthermore, while *Nos2* was unchanged (Fig. 4H), *Arg1* was lower in the contralateral PFC of SNI rats than in Sham (Fig. 4I). Similar results were also achieved in the contralateral PSC that centrally processes pain-nociception (Fig. S3B). Overall, these data provide further evidence that unlike spinal microglia/macrophages, cortical microglia/macrophages have dampened capacity to exert anti-inflammatory and phagocytic functions following SNI.

3.6. Dampened spinal microglial/macrophage pro-inflammatory activation until late stage, but attenuated mechanical allodynia mostly at early stage of SNI by chronic intrathecal minocycline treatment

To grasp whether subtypes of spinal and cortical microglia/macrophages may contribute to SNI-induced mechanical allodynia differently, we further utilized minocycline, which is known to dampen M1 microglial/macrophage polarization (Kobayashi et al., 2013). To test its potential therapeutic effect, we treated SNI rats intraperitoneally (i.p.) with minocycline starting from POD4 for 14 days (Fig. S4A), and found that although systemic minocycline treatment effectively dampened spinal microglial/macrophage pro-inflammatory activation (Fig. S4B–E), it failed to alleviate mechanical allodynia (Fig. S4F) on POD21 following SNI, suggesting that chronic systemic minocycline treatment has no therapeutic effect on existing mechanical allodynia.

We next tested whether minocycline treatment can be effective when applied to the SC locally and prophylactically. Thus, we administrated minocycline intrathecally to rats starting on the operation day before SNI surgery and continued on a daily basis for two weeks, while assessing mechanical allodynia regularly in this period (Fig. 5A). Interestingly, minocycline attenuated mechanical allodynia until POD10 but was no longer effective afterward, with the anti-allodynic effect being most prominent before POD3 (Fig. 5B). On POD9, minocycline-treated SNI rats spent more time in the center of an open field, indicating less anxiousness as compared to saline-treated rats (Fig. 5C). Importantly, minocycline dampened ipsilateral spinal MHCII$^+$ microglia/macrophages on as early as POD3 (Fig. 5D, normalized cell number shown in Fig. S5A), whereas CD172a$^+$ microglia/macrophages were unaffected (Fig. 5E, normalized cell number shown in Fig. S5B), making MHCII$^+$/CD172a$^+$ microglial/macrophage ratio lower in Mino as compared to saline group still on POD13 (Fig. 5F). However, in the PSC, it only impaired microglial/macrophage CD11b/c expression on POD3 and POD13 (Fig. S5C) but failed to dampen pro-inflammatory microglial/macrophage activation at either time point, and similarly in the PFC (both data not shown). These data demonstrated that early minocycline treatment was effective in preventing or alleviating neuropathic pain initially, but the effect was not long-lasting, even if its anti-inflammatory effect lasted longer in the SC. In light of the afore-described chronic pro-inflammatory activation of MHCII$^+$ cortical microglia/macrophages in SNI (Fig. 3B–D), whether such loss of efficacy by minocycline at late stage may be due to its inability to dampen chronic cortical microglial/macrophage activation is outstanding.

4. Discussion

In this study, we quantitatively measured the number of microglia/macrophages and characterized microglial/macrophage activation profiles in different CNS areas of adult male rats at different stages (POD3, 7 and 21) following SNI by flow cytometry. This method, in combination with other laboratorial and computational approaches, allowed us to explore the temporal-

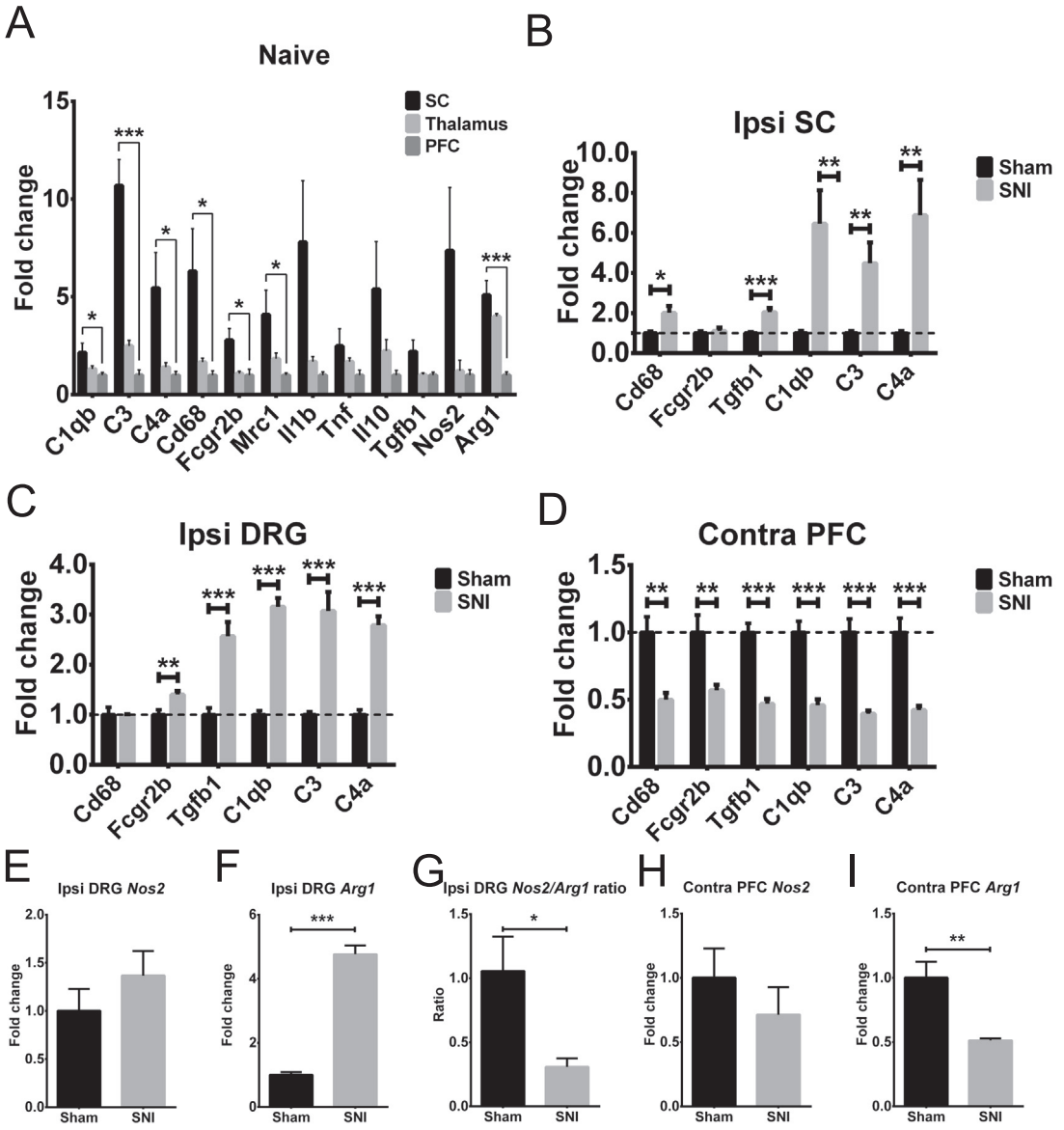

Fig. 4. Differential gene expression across the lumbar SC, thalamus and PFC of naïve rats, and in the ipsilateral lumbar SC, DRG and contralateral PFC between SNI and Sham rats on POD7. Naïve = 6, Sham = 8, SNI = 8. (A) Higher mRNA levels of *C1qb* ($F(2,15) = 3.945$, $p = 0.0420$), *C3* ($F(2,15) = 41.95$, $p < 0.0001$), *C4a* ($F(2,15) = 5.368$, $p = 0.0174$), *Cd68* ($F(2,15) = 5.252$, $p = 0.0187$), *Fcgr2b* ($F(2,15) = 7.055$, $p = 0.0069$), *Mrc1* ($F(2,15) = 4.745$, $p = 0.0253$) and *Arg1* ($F(2,15) = 22.53$, $p < 0.0001$) in the lumbar SC than the PFC of naïve rats. Significant differences between lumbar SC and PFC were marked by asterisks. (B) Higher mRNA levels of *Cd68* ($t = 2.850$, $p = 0.0146$), *Tgfb1* ($t = 4.820$, $p = 0.0003$), *C1qb* ($t = 3.264$, $p = 0.0057$), *C3* ($t = 3.357$, $p = 0.0047$) and *C4a* ($t = 3.324$, $p = 0.0050$) in the ipsi lumbar DH of SNI rats than Sham. (C) Higher mRNA levels of *Fcgr2b* ($t = 3.208$, $p = 0.0063$), *Tgfb1* ($t = 4.927$, $p = 0.0002$), *C1qb* ($t = 11.27$, $p < 0.0001$), *C3* ($t = 5.300$, $p = 0.0001$) and *C4a* ($t = 8.697$, $p < 0.0001$) in the ipsi DRG of SNI rats than Sham. (D) Lower mRNA levels of *Cd68* ($t = 3.919$, $p = 0.0015$), *Fcgr2b* ($t = 3.201$, $p = 0.0064$), *Tgfb1* ($t = 6.753$, $p < 0.0001$), *C1qb* ($t = 5.865$, $p < 0.0001$), *C3* ($t = 5.871$, $p < 0.0001$) and *C4a* ($t = 5.200$, $p = 0.0001$) in the contra PFC of SNI rats than Sham. (E-I) M1 (*Nos2*) and M2 (*Arg1*) MG/MΦ signature genes in the ipsi DRG and contra PFC were also compared. While no changes in *Nos2* were found (E & H), *Arg1* was higher (F, $t = 12.42$, $p < 0.0001$), making *Nos2*/*Arg1* ratio (G, $t = 2.870$, $p = 0.0131$) lower in the ipsi DRG of SNI rats than Sham, whereas in the contra PFC, *Arg1* (I, $t = 12.42$, $p < 0.0001$) was lower in SNI rats than Sham. Data were analyzed by a one-way ANOVA with Bonferroni's *post hoc* test or Student's *t* test and presented as mean ± SEM. $^{*}p < 0.05$, $^{**}p < 0.01$, $^{***}p < 0.001$.

spatial nature of microglia/macrophages and reveal their novel properties in neuropathic pain more deeply. To validate our flow cytometric method, we first compared it with IHC. Flow cytometry revealed significantly increased numbers of total microglia/macrophages in the ipsilateral lumbar SCs of SNI rats, which is consistent with our IHC data. Additionally, flow cytometry also detected higher levels of spinal microglial/macrophage CD11b/c expression, which is a common IHC marker for microglial/macrophage activation.

While aiming to address M1 versus M2 microglial/macrophage polarization in SNI, we intended to be cautious in using these terms due to limitation of available flow markers for a more accurate definition. Nevertheless, we regarded the MHCII^{+} microglia/macrophages as more pro-inflammatory while CD172a^{+} cells as more anti-inflammatory based on the known immunoproperties that they have respectively. In particular, CD172a is an ITIM-bearing receptor that is expressed on microglia/macrophages to restrain their pro-inflammatory activation and thus regarded as an M2 marker (Linnartz and Neumann, 2013). Surprisingly, when comparing microglial/macrophage activation profiles, we observed less abundant pro-inflammatory MHCII^{+} subtype of spinal microglia/macrophages in SNI on POD21. This observation suggests that spinal microglia/macrophages may require sufficient time to dampen their pro-inflammatory response so as to

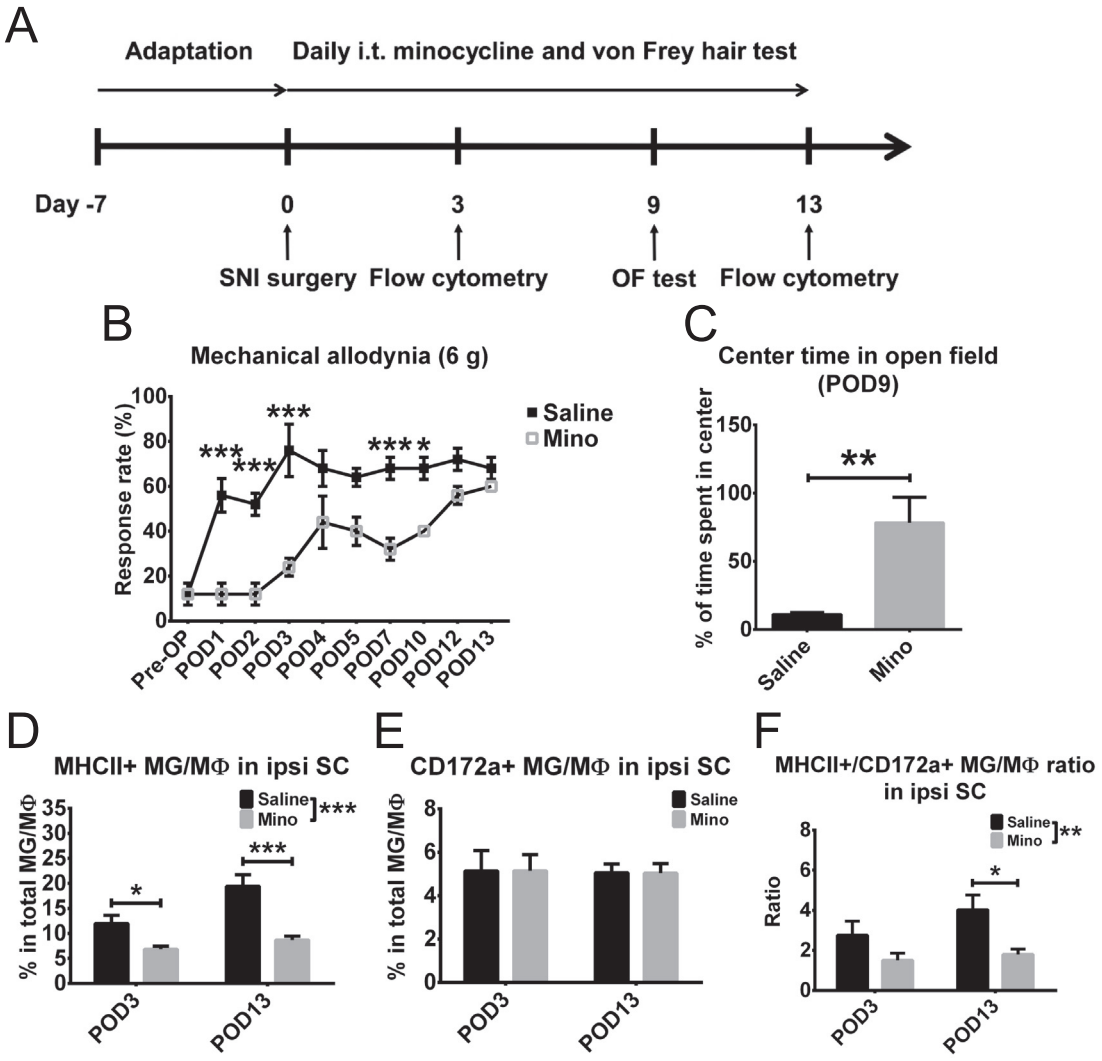

Fig. 5. Chronic intrathecal minocycline treatment dampens spinal MG/MΦ pro-inflammatory activation until late stage, but attenuates mechanical allodynia mostly at early stages of SNI. SNI rats were treated with saline or minocycline (Mino: 50 μg per day starting on POD0 for 14 consecutive days, i.t.) (POD3: Saline = 6, Mino = 5; POD13: Saline = 5, Mino = 5). (A) A flow chart illustrates the experimental procedure. (B) Measurement of ipsilateral hind paw withdrawal response rate at the stimulus force of 6 g prior to operation (Pre-OP) and afterward showed analgesic effect of minocycline treatment until POD10, with the effect most prominent before POD3 (treatment effect: $F(1,8) = 46.24$, $p = 0.0001$; time effect: $F(9,72) = 16.93$, $p < 0.0001$; group × time interaction: $F(9,72) = 4.274$, $p = 0.0002$). (C) Mino-treated SNI rats spent a higher percentage of time in the center of an open field than Saline group on POD9 ($t = 3.617$, $p = 0.0068$). (D-F) Percentages of spinal MHCII$^+$ MG/MΦ and CD172a$^+$ MG/MΦ, and MHCII$^+$/CD172a$^+$ MG/MΦ ratios were compared. The percentages of MHCII$^+$ MG/MΦ were increased in Saline but not Mino group within POD13, and were lower in the Mino than Saline group on both POD3 and POD13 (D, treatment effect: $F(1,17) = 26.85$, $p < 0.0001$; time effect: $F(1,17) = 9.179$, $p = 0.0076$), contributing to lower MHCII$^+$/CD172a$^+$ MG/MΦ ratios, particularly on POD13 (F, treatment effect: $F(1,17) = 9.061$, $p = 0.0079$). Data were analyzed by a two-way ANOVA with Fisher's LSD or Bonferroni's *post hoc* test or Student's *t* test and presented as mean ± SEM. $^*p < 0.05$, $^{**}p < 0.01$, $^{***}p < 0.001$.

adaptively exert neuroprotective and wound healing effects following SNI. Importantly, we found that early enough local minocycline treatment can accelerate dampening of MHCII$^+$ spinal microglia/macrophages at an early stage (POD3), along with alleviation of mechanical allodynia.

Intriguingly, in contrast to spinal microglia/macrophages, microglia/macrophages in the PFC showed a different response with reduced anti-inflammatory CD172a$^+$ microglia/macrophages following SNI. This was accompanied with anxiety-like behavior of SNI rats, which was in agreement with our previous finding that microglia in highly anxious animals were polarized to a pro-inflammatory subtype (Li et al., 2014). The difference between the spinal and cortical microglia/macrophages indicates that they may have region-specific immune properties. Notably, when comparing basal microglial/macrophage statuses among lumbar SC, thalamus and brain cortex in naïve rats, we found that spinal microglia/macrophages had the strongest pro-inflammatory property, whereas cortical microglia/macrophages had the weakest, in terms of expression levels of CD11b/c and MHCII, and MHCII$^+$/CD172a$^+$ microglial/macrophage ratio. A further computational analysis of microarray datasets revealed multiple immune-related genes that were expressed in a region-dependent manner. These findings suggest that firstly, the brain and SC may have fundamentally different inflammatory milieus, with the brain bearing a more robust anti-inflammatory (immune-privileged) environment than the SC in physiological condition; secondly, such basal discrepancies highly possibly underlie the differential brain versus spinal responses to SNI; thirdly and more importantly, region-specific microglia/macrophages may contribute to allodynic nociception differently at different neuropathic pain stages. The underlying mechanism for the differential immune statuses of brain versus spinal microglia/macrophages is currently unclear to us. We speculate that intrinsic programing of microglial/macrophage

differentiation during the CNS development is region-specific due to the residing neuronal environment, such as differential neuronal CD200 expression (Olson, 2010), or that the permeability of the blood-brain barrier versus blood-spinal cord barrier is different due to for example the anatomical difference in vascular arrangement (Schnell et al., 1999).

Our RT-qPCR and bioinformatic results provided some further support on the regional differences in response to SNI. Following SNI, complement activation in the SC and DRG was observed at the intermediate stage of POD7, which is in agreement with two previous reports (Griffin et al., 2007; Levin et al., 2008). Complement-activation triggers microglial/macrophage activation and subsequent phagocytosis of damaged tissue debris to exert neuroprotective functions (Linnartz and Neumann, 2013). Meanwhile, higher levels of anti-inflammatory molecules, such as the *Tgfb1*, the ITIM receptor *Fcgr2b*, and the M2 marker *Arg1*, but not pro-inflammatory genes such as the *Il1b*, *Tnf* and *Nos2*, may guarantee an appropriate inflammatory status quo of microglia/macrophages while maintaining their optimal phagocytic activities in the SC and DRG following SNI. By contrast, the PFC and PSC showed a totally opposite inflammatory response to SNI with a dampened anti-inflammatory/phagocytic phenotype. Such a phenomenon reinstates the currently recognized importance of dampening central inflammation that may exaggerate pain-sensitization at chronic stage of neuropathic pain.

Notably, the analgesic-anxiolytic and anti-inflammatory effects of minocycline that we observed in this study further highlighted the utmost importance of modulating microglia/macrophages in a region-specific as well as a cell type-specific manner to tackle inflammatory responses toward nerve injury. Minocycline has been demonstrated to specifically inhibit M1 polarization of microglia (Kobayashi et al., 2013), and has been tested in many preclinical studies of neuropathic pain, but so far with intriguingly mixed results that lack insightful explanations (Raghavendra et al., 2003; Ledeboer et al., 2005; Osikowicz et al., 2009; Chang and Waxman, 2010; Willemen et al., 2010; Sung et al., 2012; Burke et al., 2014; Taylor et al., 2015; Yamamoto et al., 2015). In our hands, a chronic daily intrathecal minocycline treatment that started early before SNI surgery effectively alleviated neuropathic pain-like and anxiety-like behaviors at early but not late postoperative stages, whereas a chronic i.p. minocycline treatment that started postoperatively was not effective at all. These results agree with several previously reported observations (Raghavendra et al., 2003; Ledeboer et al., 2005; Sung et al., 2012; Yamamoto et al., 2015), which indicate that minocycline has limited analgesic efficacy.

Most interestingly, we found that both our minocycline treatment regimes (e.g. *post hoc* i.p. and prophylactic i.t.) were effective in dampening pro-inflammatory microglial/macrophage activation in the SC, which outlasted its analgesic and anxiolytic effects, but failed to do so in the brain. This suggests that although promoting anti-inflammatory microglial/macrophage activation in the SC by minocycline is effective and important at acute stage, it may be dispensable at chronic stage, when pain-nociception becomes more centralized at the supraspinal level. At chronic stage, ascending signal from the spinal DH may prime brain microglia/macrophages toward a pro-inflammatory response, as indicated by our data. Primed pro-inflammatory brain microglia/macrophages may in turn sensitize pain e.g. by activating descending pronociceptive pathways, where intrathecal minocycline may no longer be effective enough. This complexity highlights the need of a treatment strategy that can efficiently target not only spinal but also brain inflammation in chronic neuropathic pain. Unfortunately, this was not achieved by the two minocycline regimes utilized here, as neither regime was found to efficiently dampen brain pro-inflammatory microglial/macrophage activation, which calls for a better drug candidate or treatment strategy. Nevertheless, our data offered a plausible explanation on the long-unresolved disputations of minocycline's analgesic effects and provided more insightful hints on the underlying mechanisms.

It should however be cautioned that we only characterized microglial/macrophage but not astrocytic responses in the lumbar SC and brain. It has been suggested that microglia and astrocytes in the DH play critical roles in initiation and persistence of neuropathic pain, respectively (Benarroch, 2010; Graeber and Christie, 2012). Our data could also be interpreted so that spinal microglia/macrophages may play a more critical role in pain-initiation, whereas astrocytes may be more important for pain-maintenance. This was substantiated by a previous study showing that fluorocitrate (targeting both astrocytes and microglia) was more effective in alleviating neuropathic pain than minocycline (Tanga et al., 2004). Thus, dampening spinal microglial/macrophage activation by minocycline in the chronic phase when astrocytes are already fully activated may not be effective enough, which warrants a future investigation.

In summary, we showed according to our best knowledge the first evidence that spinal and brain microglia/macrophages are functionally not the same in chronic neuropathic pain. Our data further indicated that tackling not only spinal but also brain inflammation, especially at chronic stages, shall be more powerful in alleviating chronic neuropathic pain, and offered a clue on the mechanism of anti-inflammatory analgesic-anxiolytic effect of minocycline. Our observation of region-specific microglial/macrophage profiles also rings a bell for the pain research community, as most researchers use brain-derived microglia/macrophages to mimic spinal microglia/macrophages, merely based on the fact that they are much easier to be collected and cultured and on the assumption that microglia/macrophages are homogeneous in the CNS, which is nowadays recognized not to be true based on the data provided by us and the others (Lawson et al., 1990; Savchenko et al., 1997; Olson, 2010; Doorn et al., 2015; Grabert et al., 2016).

Conflict of interest

The authors declare no conflict of interest.

Acknowledgments

This work was supported by the Academy of Finland (grant numbers 273108, 283085), National Natural Science Foundation of China (grant number 81461130016), and European Commission FP7/Cooperation sub-programme/HEALTH-2013-Innovation (grant number 602919) to LT, and Sigrid Jusélius Foundation to AP. ZL was supported by the Doctoral Program in Biomedicine at the University of Helsinki, China Scholarship Council, and Magnus Ehrnrooth Foundation. The funding sources had no role in study design, data collection and analysis, writing of the report, or decision to submit the article for publication.

Appendix A. Supplementary data

Supplementary data associated with this article can be found, in the online version, at http://dx.doi.org/10.1016/j.bbi.2016.05.021.

References

Aldskogius, H., Kozlova, E.N., 2013. Microglia and neuropathic pain. CNS Neurol. Disord.: Drug Targets 12, 768–772.

Anthony, R.M., Ravetch, J.V., 2010. A novel role for the IgG Fc glycan: the anti-inflammatory activity of sialylated IgG Fcs. J. Clin. Immunol. 30 (Suppl 1), S9–14.

Benarroch, E.E., 2010. Central neuron-glia interactions and neuropathic pain: overview of recent concepts and clinical implications. Neurology 75, 273–278.
Blackbeard, J., O'Dea, K.P., Wallace, V.C., Segerdahl, A., Pheby, T., Takata, M., Field, M. J., Rice, A.S., 2007. Quantification of the rat spinal microglial response to peripheral nerve injury as revealed by immunohistochemical image analysis and flow cytometry. J. Neurosci. Methods 164, 207–217.
Burke, N.N., Kerr, D.M., Moriarty, O., Finn, D.P., Roche, M., 2014. Minocycline modulates neuropathic pain behaviour and cortical M1–M2 microglial gene expression in a rat model of depression. Brain Behav. Immun. 42, 147–156.
Campbell, J.N., Meyer, R.A., 2006. Mechanisms of neuropathic pain. Neuron 52, 77–92.
Carson, M.J., Bilousova, T.V., Puntambekar, S.S., Melchior, B., Doose, J.M., Ethell, I.M., 2007. A rose by any other name? The potential consequences of microglial heterogeneity during CNS health and disease. Neurotherapeutics 4, 571–579.
Chang, Y.W., Waxman, S.G., 2010. Minocycline attenuates mechanical allodynia and central sensitization following peripheral second-degree burn injury. J. Pain 11, 1146–1154.
Cherry, J.D., Olschowka, J.A., O'Banion, M.K., 2014. Are "resting" microglia more "m2"? Front. Immunol. 5, 594.
Costigan, M., Moss, A., Latremoliere, A., Johnston, C., Verma-Gandhu, M., Herbert, T. A., Barrett, L., Brenner, G.J., Vardeh, D., Woolf, C.J., Fitzgerald, M., 2009. T-cell infiltration and signaling in the adult dorsal spinal cord is a major contributor to neuropathic pain-like hypersensitivity. J. Neurosci. 29, 14415–14422.
Decosterd, I., Woolf, C.J., 2000. Spared nerve injury: an animal model of persistent peripheral neuropathic pain. Pain 87, 149–158.
Doorn, K.J., Breve, J.J., Drukarch, B., Boddeke, H.W., Huitinga, I., Lucassen, P.J., van Dam, A.M., 2015. Brain region-specific gene expression profiles in freshly isolated rat microglia. Front. Cell Neurosci. 9, 84.
Echeverry, S., Shi, X.Q., Zhang, J., 2008. Characterization of cell proliferation in rat spinal cord following peripheral nerve injury and the relationship with neuropathic pain. Pain 135, 37–47.
Franco, R., Fernandez-Suarez, D., 2015. Alternatively activated microglia and macrophages in the central nervous system. Prog. Neurobiol. 131, 65–86.
Grabert, K., Michoel, T., Karavolos, M.H., Clohisey, S., Baillie, J.K., Stevens, M.P., Freeman, T.C., Summers, K.M., McColl, B.W., 2016. Microglial brain region-dependent diversity and selective regional sensitivities to aging. Nat. Neurosci. 19, 504–516.
Grace, P.M., Hutchinson, M.R., Maier, S.F., Watkins, L.R., 2014. Pathological pain and the neuroimmune interface. Nat. Rev. Immunol. 14, 217–231.
Graeber, M.B., Christie, M.J., 2012. Multiple mechanisms of microglia: a gatekeeper's contribution to pain states. Exp. Neurol. 234, 255–261.
Griffin, R.S., Costigan, M., Brenner, G.J., Ma, C.H., Scholz, J., Moss, A., Allchorne, A.J., Stahl, G.L., Woolf, C.J., 2007. Complement induction in spinal cord microglia results in anaphylatoxin C5a-mediated pain hypersensitivity. J. Neurosci. 27, 8699–8708.
Herculano-Houzel, S., 2014. The glia/neuron ratio: how it varies uniformly across brain structures and species and what that means for brain physiology and evolution. Glia 62, 1377–1391.
Herrera-Molina, R., von Bernhardi, R., 2005. Transforming growth factor-beta 1 produced by hippocampal cells modulates microglial reactivity in culture. Neurobiol. Dis. 19, 229–236.
Hu, X., Liou, A.K., Leak, R.K., Xu, M., An, C., Suenaga, J., Shi, Y., Gao, Y., Zheng, P., Chen, J., 2014. Neurobiology of microglial action in CNS injuries: receptor-mediated signaling mechanisms and functional roles. Prog. Neurobiol. 119–120, 60–84.
Hu, X., Leak, R.K., Shi, Y., Suenaga, J., Gao, Y., Zheng, P., Chen, J., 2015. Microglial and macrophage polarization-new prospects for brain repair. Nat. Rev. Neurol. 11, 56–64.
Kasymov, V., Larina, O., Castaldo, C., Marina, N., Patrushev, M., Kasparov, S., Gourine, A.V., 2013. Differential sensitivity of brainstem versus cortical astrocytes to changes in pH reveals functional regional specialization of astroglia. J. Neurosci. 33, 435–441.
Kobayashi, K., Imagama, S., Ohgomori, T., Hirano, K., Uchimura, K., Sakamoto, K., Hirakawa, A., Takeuchi, H., Suzumura, A., Ishiguro, N., Kadomatsu, K., 2013. Minocycline selectively inhibits M1 polarization of microglia. Cell Death Dis. 4, e525.
Komori, T., Morikawa, Y., Inada, T., Hisaoka, T., Senba, E., 2011. Site-specific subtypes of macrophages recruited after peripheral nerve injury. NeuroReport 22, 911–917.
Lawson, L.J., Perry, V.H., Dri, P., Gordon, S., 1990. Heterogeneity in the distribution and morphology of microglia in the normal adult mouse brain. Neuroscience 39, 151–170.
Ledeboer, A., Sloane, E.M., Milligan, E.D., Frank, M.G., Mahony, J.H., Maier, S.F., Watkins, L.R., 2005. Minocycline attenuates mechanical allodynia and proinflammatory cytokine expression in rat models of pain facilitation. Pain 115, 71–83.
Levin, M.E., Jin, J.G., Ji, R.R., Tong, J., Pomonis, J.D., Lavery, D.J., Miller, S.W., Chiang, L. W., 2008. Complement activation in the peripheral nervous system following the spinal nerve ligation model of neuropathic pain. Pain 137, 182–201.
Li, Z., Ma, L., Kulesskaya, N., Voikar, V., Tian, L., 2014. Microglia are polarized to M1 type in high-anxiety inbred mice in response to lipopolysaccharide challenge. Brain Behav. Immun. 38, 237–248.
Linnartz, B., Neumann, H., 2013. Microglial activatory (immunoreceptor tyrosine-based activation motif)- and inhibitory (immunoreceptor tyrosine-based inhibition motif)-signaling receptors for recognition of the neuronal glycocalyx. Glia 61, 37–46.
McMahon, S.B., Russa, F.L., Bennett, D.L., 2015. Crosstalk between the nociceptive and immune systems in host defence and disease. Nat. Rev. Neurosci. 16, 389–402.
Milligan, E.D., Watkins, L.R., 2009. Pathological and protective roles of glia in chronic pain. Nat. Rev. Neurosci. 10, 23–36.
Nicholson, B., Verma, S., 2004. Comorbidities in chronic neuropathic pain. Pain Med. 5 (Suppl. 1), S9–S27.
Okuneva, O., Korber, I., Li, Z., Tian, L., Joensuu, T., Kopra, O., Lehesjoki, A.E., 2015. Abnormal microglial activation in the Cstb(−/−) mouse, a model for progressive myoclonus epilepsy, EPM1. Glia 63, 400–411.
Olson, J.K., 2010. Immune response by microglia in the spinal cord. Ann. N. Y. Acad. Sci. 1198, 271–278.
Osikowicz, M., Skup, M., Mika, J., Makuch, W., Czarkowska-Bauch, J., Przewlocka, B., 2009. Glial inhibitors influence the mRNA and protein levels of mGlu2/3, 5 and 7 receptors and potentiate the analgesic effects of their ligands in a mouse model of neuropathic pain. Pain 147, 175–186.
Page, G.G., Opp, M.R., Kozachik, S.L., 2014. Reduced sleep, stress responsivity, and female sex contribute to persistent inflammation-induced mechanical hypersensitivity in rats. Brain Behav. Immun. 40, 244–251.
Popiolek-Barczyk, K., Kolosowska, N., Piotrowska, A., Makuch, W., Rojewska, E., Jurga, A.M., Pilat, D., Mika, J., 2015. Parthenolide relieves pain and promotes M2 microglia/macrophage polarization in rat model of neuropathy. Neural Plast. 2015, 676473.
Raghavendra, V., Tanga, F., DeLeo, J.A., 2003. Inhibition of microglial activation attenuates the development but not existing hypersensitivity in a rat model of neuropathy. J. Pharmacol. Exp. Ther. 306, 624–630.
Ransohoff, R.M., Cardona, A.E., 2010. The myeloid cells of the central nervous system parenchyma. Nature 468, 253–262.
Saijo, K., Glass, C.K., 2011. Microglial cell origin and phenotypes in health and disease. Nat. Rev. Immunol. 11, 775–787.
Savchenko, V.L., Nikonenko, I.R., Skibo, G.G., McKanna, J.A., 1997. Distribution of microglia and astrocytes in different regions of the normal adult rat brain. Neurophysiology 29, 343–351.
Schitine, C., Nogaroli, L., Costa, M.R., Hedin-Pereira, C., 2015. Astrocyte heterogeneity in the brain: from development to disease. Front. Cell Neurosci. 9, 76.
Schnell, L., Fearn, S., Klassen, H., Schwab, M.E., Perry, V.H., 1999. Acute inflammatory responses to mechanical lesions in the CNS: differences between brain and spinal cord. Eur. J. Neurosci. 11, 3648–3658.
Sung, C.S., Cherng, C.H., Wen, Z.H., Chang, W.K., Huang, S.Y., Lin, S.L., Chan, K.H., Wong, C.S., 2012. Minocycline and fluorocitrate suppress spinal nociceptive signaling in intrathecal IL-1beta-induced thermal hyperalgesic rats. Glia 60, 2004–2017.
Tanga, F.Y., Raghavendra, V., DeLeo, J.A., 2004. Quantitative real-time RT-PCR assessment of spinal microglial and astrocytic activation markers in a rat model of neuropathic pain. Neurochem. Int. 45, 397–407.
Taylor, A.M., Castonguay, A., Taylor, A.J., Murphy, N.P., Ghogha, A., Cook, C., Xue, L., Olmstead, M.C., De Koninck, Y., Evans, C.J., Cahill, C.M., 2015. Microglia disrupt mesolimbic reward circuitry in chronic pain. J. Neurosci. 35, 8442–8450.
Tsuda, M., Masuda, T., Tozaki-Saitoh, H., Inoue, K., 2013. Microglial regulation of neuropathic pain. J. Pharmacol. Sci. 121, 89–94.
Willemen, H.L., Eijkelkamp, N., Wang, H., Dantzer, R., Dorn 2nd, G.W., Kelley, K.W., Heijnen, C.J., Kavelaars, A., 2010. Microglial/macrophage GRK2 determines duration of peripheral IL-1beta-induced hyperalgesia: contribution of spinal cord CX3CR1, p38 and IL-1 signaling. Pain 150, 550–560.
Xu, F., Huang, J., He, Z., Chen, J., Tang, X., Song, Z., Guo, Q., Huang, C., 2016. Microglial polarization dynamics in dorsal spinal cord in the early stages following chronic sciatic nerve damage. Neurosci. Lett. 617, 6–13.
Yamamoto, Y., Terayama, R., Kishimoto, N., Maruhama, K., Mizutani, M., Iida, S., Sugimoto, T., 2015. Activated microglia contribute to convergent nociceptive inputs to spinal dorsal horn neurons and the development of neuropathic pain. Neurochem. Res. 40, 1000–1012.